



**DEPARTURE THROUGHPUT STUDY  
FOR BOSTON LOGAN INTERNATIONAL AIRPORT**

Ioannis Simaiakis and Hamsa Balakrishnan

Report No. ICAT-2011-1  
January 2011

MIT International Center for Air Transportation (ICAT)  
Department of Aeronautics & Astronautics  
Massachusetts Institute of Technology  
Cambridge, MA 02139 USA

## **Abstract**

We propose a new parametric representation of the departure capacity of airports. In particular, we show how the departure capacity can be represented by the variation of the average departure throughput as a function of arrivals, conditioned on persistent departure demand. We also show how this approach can be extended to quantify the dependence of departure capacity on other parameters such as the fleet mix. The proposed approaches are illustrated through the parametric estimation of the departure capacity of Boston Logan International Airport (BOS).

# Contents

<b>1</b>	<b>Introduction</b>	<b>3</b>
<b>2</b>	<b>Average departure throughput</b>	<b>3</b>
<b>3</b>	<b>Departure throughput as a function of departure demand and arrival throughput</b>	<b>5</b>
3.1	Variance of the departure throughput . . . . .	7
3.2	Estimation of the saturation point $N^*$ and the average departure throughput under continuous demand . . . . .	8
<b>4</b>	<b>Estimation of the impact of fleet mix</b>	<b>9</b>
4.1	Estimation of departure capacity as a function of arrival throughput and fleet mix .	13
4.2	Comparison to capacity envelopes . . . . .	14
4.3	Interactions between jet and pro departures . . . . .	14
<b>5</b>	<b>Jet Departure Throughput</b>	<b>16</b>
5.1	Estimation of the saturation point $N_J^*$ . . . . .	16
5.2	Jet departure throughput as a function of jet departure demand and arrival throughput	17
5.3	Average jet departure throughput as a function of arrival throughput and fleet mix under persistent jet departure demand . . . . .	17
<b>6</b>	<b>Conclusions</b>	<b>18</b>

# 1 Introduction

This work focuses on parametrically estimating and representing the departure capacity of the runway system of an airport. For the purposes of this work, the departure capacity of the runway system is defined as the average number of departures that can be performed on the runway system in the presence of persistent demand conditioned on relevant parameters, such as landings, runway crossings, fleet mix etc. We show that this parametric measurement of the departure capacity explains some of the variation in the departure process. The unexplained variance is due to factors such as controller strategies, their performance, unexpected events, and other unaccounted disturbances to the system.

We illustrate the proposed approaches for runway configuration (22L, 27 | 22L, 22R) at Boston Logan International Airport (BOS) under VMC. ASPM and Flightstats data from 2007 were used for the analysis. All estimation problems were formulated as convex optimization problems and were solved using the CVX MATLAB-based modeling system.

## 2 Average departure throughput

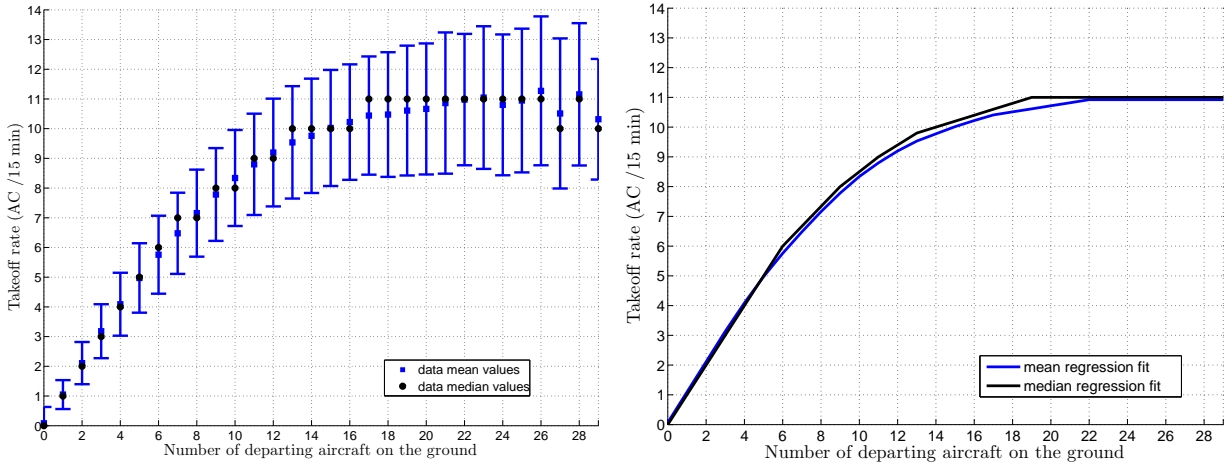
The starting point for departure throughput estimation is the representation of the departure throughput (or takeoff rate) as a function of departure demand. The departure demand,  $N(t)$ , at some time  $t$  (represented in 1-min increments) is measured as the number of aircraft taxiing out during that time interval. In other words, it is the number of aircraft that have pushed back, but not taken off yet. The departure throughput during a 15-minute period starting at time  $t$  is defined as the takeoff rate  $\bar{T}(t)$  over this time period, and is measured as the number of aircraft that took off during the 15-minute interval  $[t, t + 14]$  min.

This representation yields the plots in Figure 1a for the most frequently used runway configuration (22L, 27 | 22L, 22R) at BOS in 2007 under VMC. For the entire year, we have 121,414 data points,  $(N, \bar{T})$ . In Figure 1a (left), we plot the mean and median takeoff rate for each value of the departure demand,  $N$ . The error bars depict the standard deviation of the takeoff rate at each value of  $N$ . As  $N(t)$  increases, the takeoff rate initially increases, but then saturates at a critical value  $N^*$ . From Figure 1a, we can infer that  $N^*$  is around 20 AC and that the average takeoff rate in saturation is around 11 AC /15 minutes.

We can formalize the estimation of the mean and median throughput rate as a function of the departure demand by formulating the estimation problem as a regression problem. The function  $f$  to be fitted has to adhere to the physics of the system:

- Departure throughput is a monotonically non-decreasing function of departure demand.
- Departure throughput is a concave function of departure demand.

The estimation problem can be formulated as a least-squares problem: Given  $m$  pairs of mea-



(a) Measurements of the takeoff rate as function of the number of departing aircraft on the ground (b) Regression of the takeoff rate as function of the number of departing aircraft on the ground

Figure 1: BOS throughput in segment (VMC ; 22L, 27 | 22L, 22R)

measurements  $N(t)$  and  $T(t)$ , denoted  $(u_1, y_1), \dots, (u_m, y_m)$  for all time, we seek a non-decreasing, concave function  $f : \mathbb{R} \rightarrow \mathbb{R}$  that estimates the mean  $\bar{T} = f(N)$ . This infinite-dimensional problem gets significantly simplified by the fact that we have measurements only for discrete values of  $N(t)$  and thus  $f$ . We only need to estimate the points  $f(0), f(1), \dots, f(n)$ , where  $n = \max(N(t))$ . The function  $f$  is therefore simply a piecewise linear function of  $N$ , and the monotonicity and concavity constraints are imposed at the points  $0, 1, \dots, \max(N(t))$  by comparing the values and the slopes of subsequent pieces.  $\bar{T}$  is given by the solution to the simple convex optimization problem:

$$\min \sum_{i=1}^m (\hat{y}_i - y_i)^2 \quad (1)$$

subject to:

$$\hat{y}_i = f(u_i), \quad i = 1, \dots, m \quad (2)$$

$$f(i+1) \geq f(i), \quad i = 0, \dots, (n-1) \quad (3)$$

$$f(i+1) - f(i) \leq f(i) - f(i-1), \quad i = 1, \dots, (n-1) \quad (4)$$

Similarly, the median estimation problem is formulated as:

$$\min \sum_{i=1}^m |\hat{y}_i - y_i| \quad (5)$$

subject to:

$$\hat{y}_i = f(u_i), \quad i = 1, \dots, m \quad (6)$$

$$f(i+1) \geq f(i), \quad i = 0, \dots, (n-1) \quad (7)$$

$$f(i+1) - f(i) \leq f(i) - f(i-1), \quad i = 1, \dots, (n-1) \quad (8)$$

The results of the regression fit can be seen in Figure 1b. The mean takeoff rate saturates at 11 takeoffs/15 minutes when  $N \geq 22$  and median takeoff rate saturates at the same value when  $N \geq 19$ . We can conclude that the average takeoff rate of this runway configuration under persistent demand is 11 takeoffs per 15 minutes, or 44 takeoffs per hour. Persistent demand is achieved when the number of taxiing out aircraft is around 20.

Finally, we note that this framework can be easily extended to find estimates of upper quantiles by formulating the quantile regression, as described in [3], as a convex optimization problem:

$$\min \sum_{i=1}^m ((1-p) \cdot \max(\hat{y}_i - y_i, 0) + p \cdot \max(-\hat{y}_i + y_i, 0)) \quad (9)$$

subject to:

$$\hat{y}_i = f(u_i), \quad i = 1, \dots, m \quad (10)$$

$$f(i+1) \geq f(i), \quad i = 0, \dots, (n-1) \quad (11)$$

$$f(i+1) - f(i) \leq f(i) - f(i-1), \quad i = 1, \dots, (n-1) \quad (12)$$

Here,  $p$  takes the value of the quantile we are interested to estimate: for the median it is 0.5, for the 90% percentile 0.9, etc.

### 3 Departure throughput as a function of departure demand and arrival throughput

The method described above can be extended to represent departure throughput as a two variable function of both departure demand and arrival throughput. The arrival throughput,  $\bar{A}(t)$ , is measured as the number of landings in the 15 minute interval  $[t, t+14]$ . In other words, we represent the departure throughput,  $\bar{T}(t)$ , in the 15 minute interval  $[t, t+14]$  as a function of both the departure demand  $N(t)$  at time  $t$  and the arrival throughput,  $\bar{A}(t)$ , in the same 15 minute interval  $[t, t+14]$ . The 2-variable fitting problem has additional constraints, resulting from the physics of the system:

- For a fixed departure demand, the departure throughput is a monotonically non-increasing, concave function of the arrival throughput following the principle of capacity envelopes.
- For any value of arrival throughput, the departure throughput as a function of departure demand cannot increase at a higher rate than for a lower value of arrival throughput.
- For any value of departure demand, the departure throughput as a function of arrival through-

put cannot decrease at a lower rate than for a lower value of departure demand.

The problem is formulated similarly to the two-dimensional one: Given  $m$  triples of measurements  $N(t)$ ,  $\bar{A}(t)$  and  $\bar{T}(t)$ , denoted by  $(u_1, v_1, y_1), \dots, (u_m, v_m, y_m)$ , at all times, we seek a function  $g : \mathbb{R}^2 \rightarrow \mathbb{R}$  that estimates the mean  $\bar{T} = g(N, \bar{A}(t))$ . This infinite-dimensional problem gets again simplified by the fact that we have measurements only for discrete values of  $N(t)$ ,  $\bar{A}(t)$  and thus  $g$ . We only need to estimate the points  $g(0, 0), g(0, 1), \dots, g(n, l)$ , where  $n = \max(N(t))$ ,  $l = \max(\bar{A}(t))$ . Thus, function  $g$  is a piecewise linear function of  $\bar{A}(t)$  and  $T$ . The constraints are imposed only between neighboring points, as was done in the 2D case, but are more complex:

$$\min \sum_{i=1}^m (\hat{y}_i - y_i)^2 \quad (13)$$

subject to:

$$\hat{y}_i = g(u_i, v_i), \quad i = 1, \dots, m \quad (14)$$

$$g(i+1, j) \geq g(i, j), \quad i = 0, \dots, (n-1), \forall j \quad (15)$$

$$g(i+1, j) - g(i, j) \leq g(i, j) - g(i-1, j), \quad i = 1, \dots, (n-1), \forall j \quad (16)$$

$$g(i, j+1) \leq g(i, j), \quad j = 0, \dots, (l-1), \forall i \quad (17)$$

$$g(i, j+1) - g(i, j) \leq g(i, j) - g(i, j-1), \quad j = 1, \dots, (l-1), \forall i \quad (18)$$

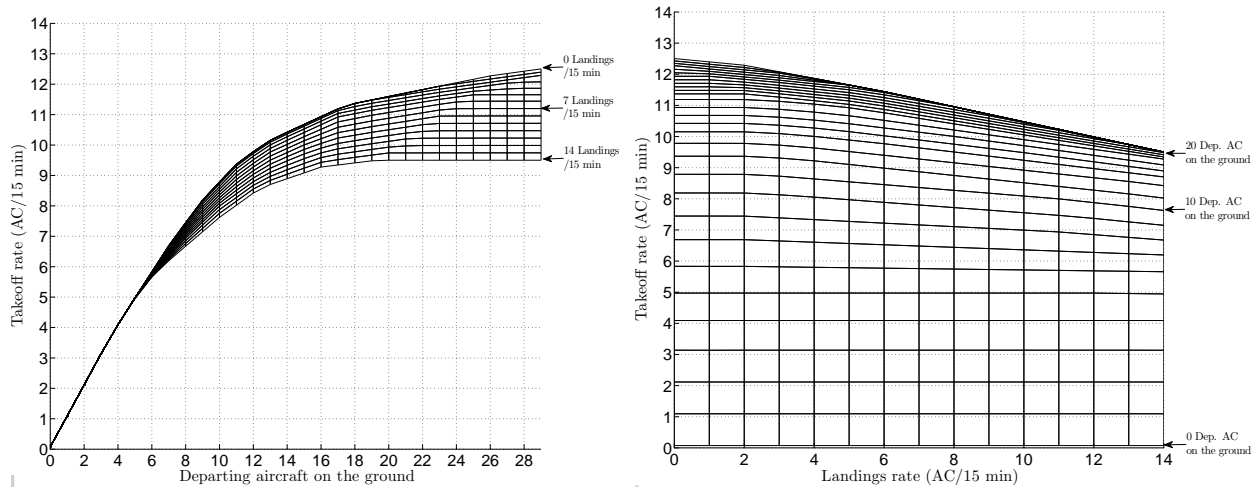
$$g(i+1, j) - g(i, j) \geq g(i+1, j+1) - g(i, j+1), \quad i = 0, \dots, (n-1), j = 0, \dots, (l-1) \quad (19)$$

$$g(i, j) - g(i, j+1) \leq g(i+1, j) - g(i+1, j+1), \quad i = 0, \dots, (n-1), j = 0, \dots, (l-1) \quad (20)$$

Inequalities 15-16 are analogous to the ones in the 2D case: For a fixed arrival throughput, the departure throughput is a monotonically non-decreasing, concave function of the departure demand. Inequalities 17-18 ensure that for fixed departure demand, the departure throughput is a non-increasing, concave function of the arrival throughput following the principle of capacity envelopes. Finally, Equation 19 ensures that the marginal gain in departure throughput from increasing the departure demand for one unit increases as the arrival throughput decreases, and Equation 20 ensures that the marginal gain in departure throughput from decreasing the arrival throughput for one unit decreases as the departure demand decreases.

Under these assumptions, the departure throughput is estimated as a function of the departure demand and arrival throughput. Two visualizations of the estimated function  $g$  can be seen in Figure 2. Figure 2a is essentially the mean regression curve of Figure 1b parameterized for different levels of arrival throughput. As expected, the arrival throughput impacts the departure throughput. Figure 2b displays the same graph from a different angle: the arrival throughput is the variable on the  $x$ -axis and the departure demand is a parameter. We observe that the trade between arrival throughput and departure throughput changes with the departure demand. We also note that for

high values of departure demand, the departure runway(s) are under persistent demand and so the curves for values of  $N$  coincide and envelop all average departure throughput data points. Thus, this envelope can be also interpreted as the capacity envelope for this runway configuration: It shows the average departure throughput under high departure demand as a function of arrivals.



(a) Takeoff rate as function of departure demand

(b) Takeoff rate as function of landings rate

Figure 2: BOS departure throughput in segment (VMC ; 22L, 27 | 22L, 22R) as function of arrivals and departure demand

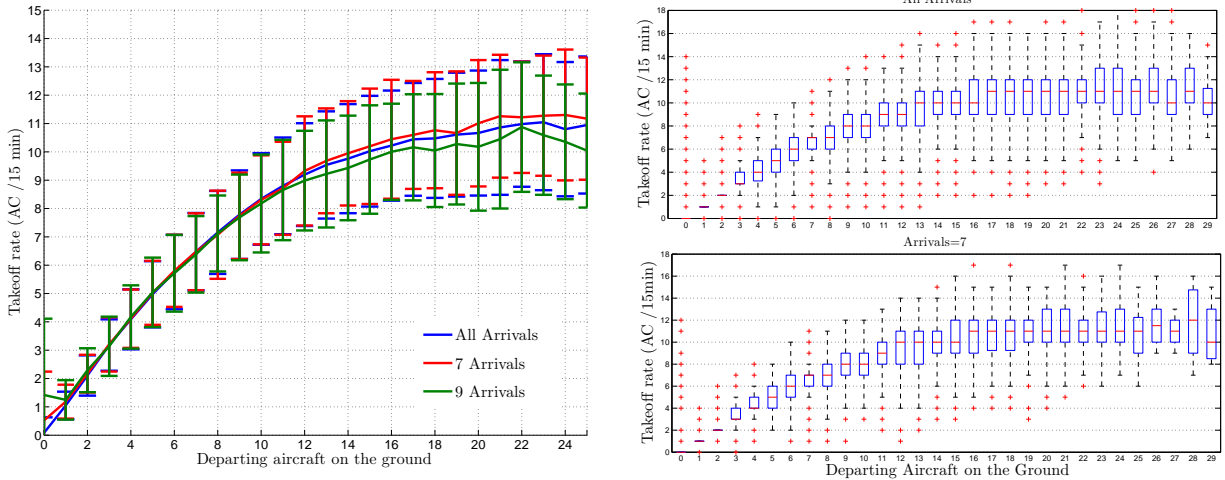
### 3.1 Variance of the departure throughput

It could be hypothesized that the high variance of the departure throughput which can be seen in Figure 1a can be explained by the (hidden) arrival throughput variable, and that by controlling for the arrival throughput variable, the variance of the departure throughput would decrease significantly. In order to informally inspect this hypothesis, we plot the departure throughput as a function of departure demand for two frequent values of arrival throughput overlaid with the departure throughput for all values of arrival throughput in Figure 3a. We observe that the variance of the departure throughput remains high even at individual arrival throughput values. In Figure 3b, we visualize the boxplots of the throughput measurements grouped for every value of the departure demand for 7 arrivals and for all arrivals. From the boxplots we observe that the 25th and 75th percentiles are spread over a range of 3 AC/15 minutes for both cases under high departure demand.

These results suggest that the observed variance of the departure throughput needs to be explained by other variables. Three potential candidates are:

- Fleet mix





(a) Mean and standard deviation of takeoff rate as function of departures demand for different numbers of landings (b) Boxplots of takeoff rate as function of departures demand for different numbers of landings

Figure 3: BOS throughput in segment (VMC ; 22L, 27 | 22L, 22R) for different numbers of landings

- Human factors (controller performance, pilot response times)
- Unexpected incidents (runway closures, mechanical failures, etc.)

Currently, we do not have data on the human factors and unexpected incidents variables, and so we focus on examining the impact of fleet mix on the departure throughput. This analysis is presented in Section 4.

### 3.2 Estimation of the saturation point $N^*$ and the average departure throughput under continuous demand

Traditional statistical methods for the problem of predicting the response variable (departure throughput) as a function of several independent variables (departure demand, arrival throughput, fleet mix) would make hard to exploit the structure of the problem and impose the constraints that result from the physics of the system. For this reason, we follow a different approach: We isolate instances of high departure demand, and then estimate the departure throughput as a function of the arrival throughput and the fleet mix. To this end, we need to estimate the threshold  $N^*$  at which the departure throughput stops varying with departure demand. There are several ways to estimate  $N^*$ , for example, through the inspection of Figure 1a or Figure 1b. Both plots suggest that the mean throughput saturates at  $N^* = 22$ .

A more robust way to identify  $N^*$  is to group the throughput observations of each value of  $N$  and use a non-parametric method to test for significant differences between the throughput observations of each group. More specifically we use the Kruskal-Wallis one-way analysis of variance. The test

does not reject the null-hypothesis that the throughput observations at different values of  $N$  are drawn from the same distribution at both 0.05 and 0.1 significance levels for  $N \geq 22$ . However, it does reject the null hypothesis if we include more groups at lower values of  $N$ . The test implies that the measurements of throughput for different values of  $N \geq 22$  are not significantly different. As we can see, the different methods lead to the same conclusion: All else being equal, the departure throughput does not significantly change with departure demand at demand values greater than or equal to 22. In other words,  $N^* = 22$ . We can now isolate all data points for which  $N \geq 22$  and study the explanatory power of other variables.

As a first step, we use the data points for which  $N \geq N^*$  to plot the average departure throughput as a function of arrival throughput, and estimate the least square fit of a concave non-increasing function to the data. Given  $k$  pairs of measurements  $\bar{A}(t)$  and  $\bar{T}(t)$ , denoted  $(v_1, y_1), \dots, (v_k, y_k)$  at all times when  $N \geq N^*$ , we seek a non-increasing, concave function  $h : \mathbb{R} \rightarrow \mathbb{R}$  that estimates the mean  $\bar{T} = h(\bar{A}(t)|N \geq N^*)$ . Again, we only need to estimate the points  $h(0), h(1), \dots, h(l)$ , where  $l = \max(\bar{A}(t))$ . Thus, function  $h$  is a piecewise linear function of  $A$  and the monotonicity and concavity constraints are imposed at the points  $0, 1, \dots, l$  by comparing the values and the slopes of subsequent pieces. The formulation of this estimation problem is as follows:

$$\min \sum_{i=1}^k (\hat{y}_i - y_i)^2 \quad (21)$$

subject to:

$$\hat{y}_i = h(v_i), \quad i = 1, \dots, k \quad (22)$$

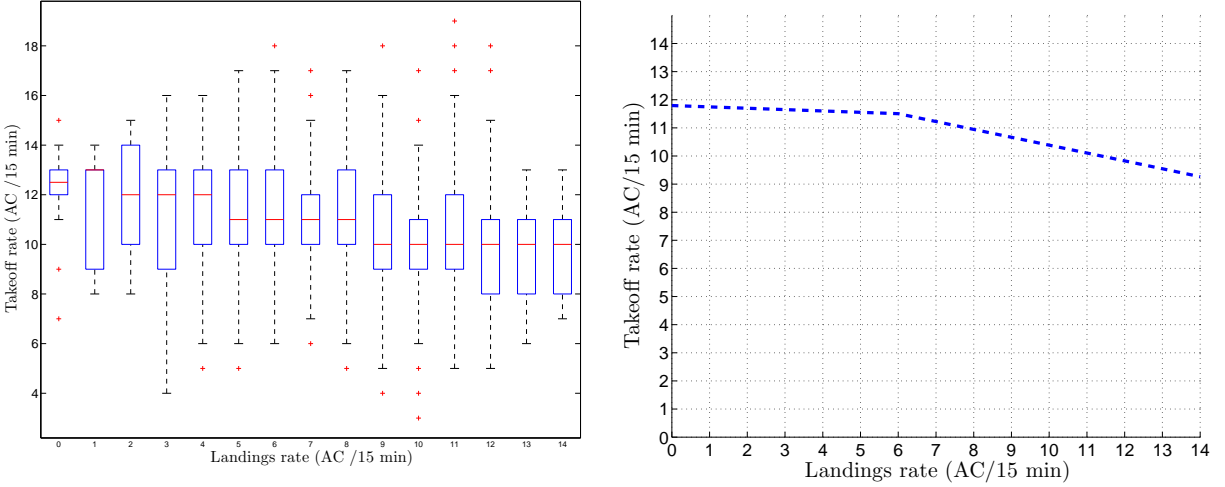
$$h(i+1) \leq h(i), \quad i = 0, \dots, (l-1) \quad (23)$$

$$h(i+1) - h(i) \leq h(i) - h(i-1), \quad i = 1, \dots, (l-1) \quad (24)$$

The boxplot of the departure throughput, grouped for every value of the arrival throughput, can be seen in Figure 4a, and the corresponding fitted function is shown in Figure 4b. The plot of Figure 4b provides a robust estimate of the average departure throughput as a function of the arrival throughput under persistent departure demand ( $N \geq N^*$ ).

## 4 Estimation of the impact of fleet mix

In order to estimate the impact of fleet mix, we continue working with the data points for which  $N \geq N^*$ . We address the problem of estimating the departure throughput as a function of the arrivals and the fleet mix. The fleet mix is not a simple numerical variable like the number of arrivals, its impact is highly dependent on the particulars of each airport (such as, runway configuration, sequencing decisions, airspace design, and local procedures). For runway configuration (22L, 27 | 22L, 22R) at BOS, given operational information from controllers, our hypothesis is that the fleet



(a) Boxplot of takeoff rate as function of landings rate for  $N \geq 22$  (b) Regression of the takeoff rate as function of landings rate for  $N \geq 22$

Figure 4: BOS departure throughput in segment (VMC ; 22L, 27 | 22L, 22R) as a function of arrivals, for  $N \geq 22$

mix can be represented with two variables:

- Number of propeller-powered aircraft ( $PDeps$ ) in the mix that is taking off in the 15-minute interval.
- Number of heavy aircraft ( $HDeps$ ) in the mix that is taking off in the 15-minute interval.

The props are fanned in between jet departures and are thus expected to increase the departure throughput. The heavy aircraft introduce longer separation requirements, and are expected to decrease the departure throughput. Based on this discussion we attempt to model the response variable, departure throughput ( $Departures$ ) in each 15-minute time interval  $[t, t+14]$ , as a function of four potential explanatory variables:

1. Number of departing aircraft on the ground at time  $t$  ( $DepDem$ )<sup>1</sup>
2. Number of landings in the 15 minute interval ( $Arrivals$ )
3. Number of props taking off in the 15-minute time interval ( $PDeps$ )
4. Number of heavy aircraft taking off in the 15-minute time interval ( $HDeps$ )

Prior to the analysis of this multi-variable estimation problem, we note that the variables  $PDeps$ ,  $HDeps$ , as we defined them, introduce a bias in the estimation problem. We illustrate

---

<sup>1</sup>Although we have established that the departure throughput does not change significantly with the number of aircraft on the ground, when  $N \geq N^*$ , it is useful to revisit this hypothesis in a more complex multi-variable model.

this bias with an example. When we estimate the departure throughput in a 15-minute interval during which 5 heavy departures were reported, what we really intend to measure is the following: how does the throughput of the airport get impacted when 5 aircraft in the front positions of the departure queue are heavy? However, we only measure the throughput of the airport given that five heavy departures were recorded. The fact that we control for the number of departures on the ground does not remove this bias. Some of the time intervals in the measurements are bound to include rare events such as a runway closure because of some unexpected incident, or the mechanical failure of some aircraft. However, the time interval in which 5 heavy departures took place is bound to be free of those rare events, otherwise 5 heavy departures would not be feasible.

We considered solving this problem by using other variables to measure the impact of fleet mix, such as the number of departing props on the ground and the number of departing heavy jets on the ground. It turned out that the most robust way to reduce the measurement bias was to remove from the data set the 15-minute intervals during which the total departure throughput is lower than the highest prop throughput, and the highest heavy aircraft throughput recorded in any 15-minute interval. In this way, we removed time intervals with exceptionally few operations. We did not remove these points in Section 3, because we wanted the average throughput curves to take into account moments of unexpectedly low throughput.

We analyze the correlations between all the variables in the model. For that we use the *pairs* function of the R programming language which produces panels with the correlations among all variables of the model. Each panel shows the scatterplot between the variable on the vertical axis and the variable on the horizontal axis as well as the lowess<sup>2</sup> curve, in red color, through a set of data points. Lowess fits follow the general trend of the data and so they are a good measure of the correlation between the two variables [1]. The response variable *Departures* is shown on the *y*-axis of the top row of the panels.

From Figure 5, we can observe that:

- The lowess fit line for the variable pair (*DepDem*, *Departures*) does not exhibit any large or systematic deviance from the  $y = 11$  line. This is further evidence that  $N^*$  was calculated correctly, and that for  $N \geq N^*$ , there is no correlation between the departures demand and the departure throughput. The departure throughput is shown to be stable at 11 AC/15 min, the same value that was calculated using the estimation method of Figure 1b.
- The lowess fit line for the variable pair (*Arrivals*, *Departures*) follows the same trend as the curve of Figure 4b: It shows that the departure throughput drops from 12 to 9 as a concave function of the arrival throughput.
- The lowess fit line for the variable pair (*Heavies*, *Departures*) exhibits a rather unclear, humped trend. The curve initially increases from 10.5 to 11 and then decreases and stabilizes

---

<sup>2</sup>locally weighted scatterplot smoothing

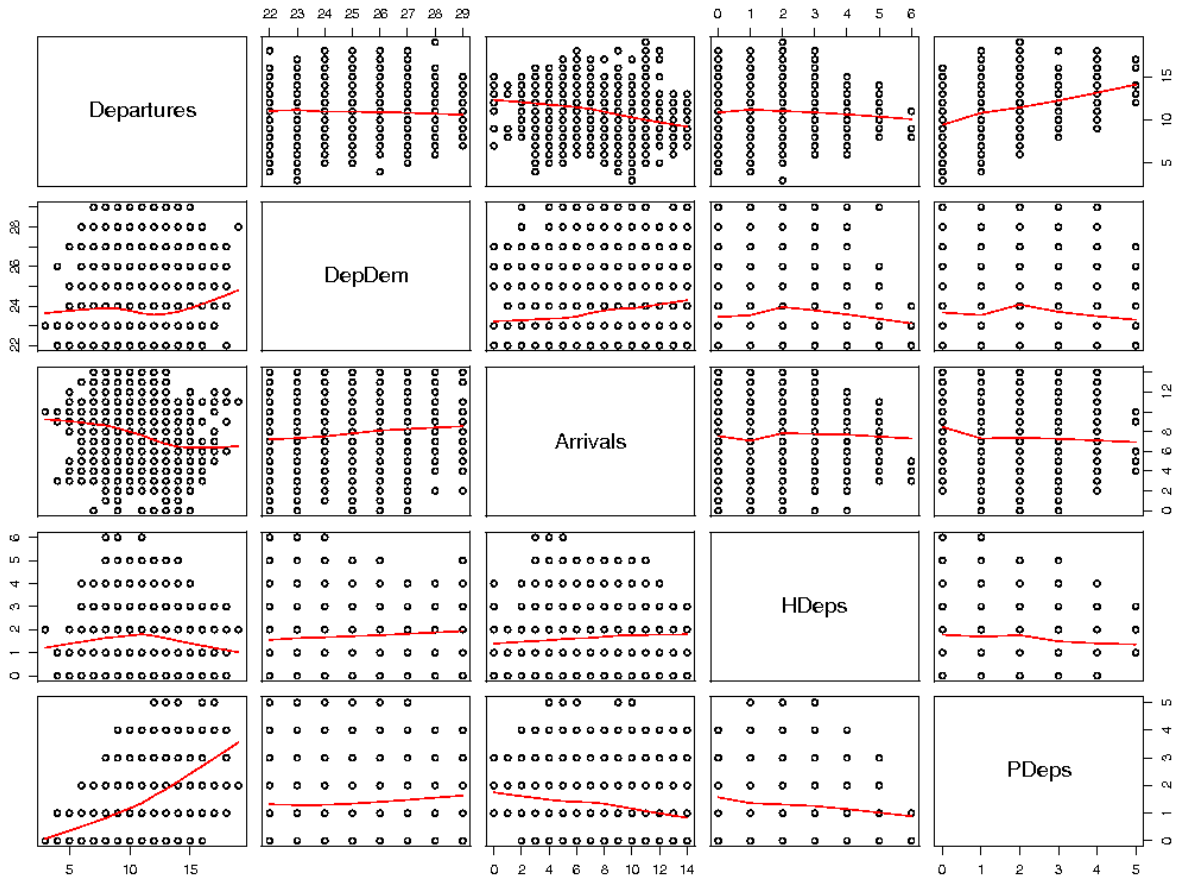


Figure 5: Correlations between Departures, Departure Demand, Arrivals, Heavy Departures and Prop Departures

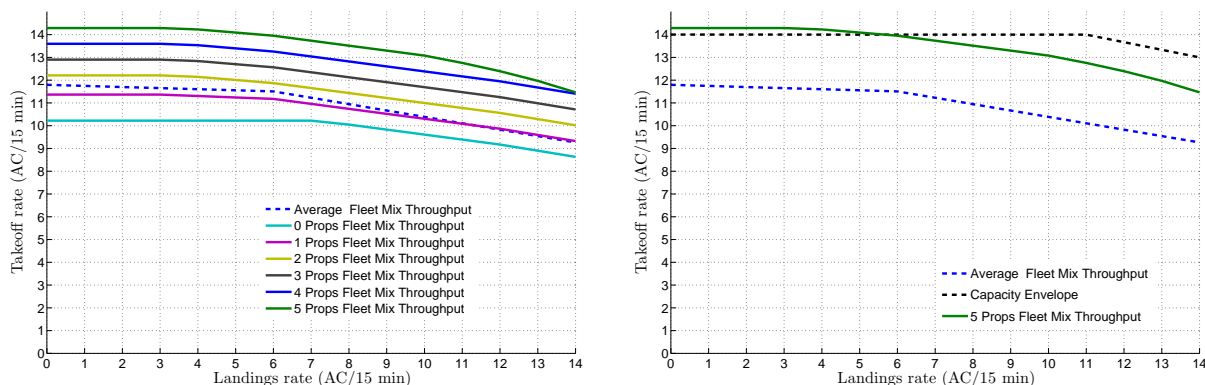
at around 10.

- The lowest fit line for the variable pair  $(DepDem, Departures)$  exhibit a clear positive correlation between the two: As the number of departures of props increases from 0 to 6 the total departure throughput appears to increase from 9 to 14.

The relationship between the departure throughput and these four variables is also examined with advanced statistical tools such as regression trees, random forests and generalized additive models. They all lead to the same conclusion: the two most significant explanatory variables are the arrivals and the prop departures. The departures of heavy aircraft do not seem to significantly impact the departure throughput. This might be surprising, but it can be explained by the operational procedures at BOS: Controllers use the high wake vortex separation requirement between a heavy and a subsequent departure to do runway crossings, and so the impact of a heavy departure on throughput may be insignificant.

## 4.1 Estimation of departure capacity as a function of arrival throughput and fleet mix

Having established that at  $N \geq N^*$  the departure throughput is primarily a function of arrivals and prop departures, we estimate this function using the approach described in Section 3. The plot of the estimated function,  $h_p(\bar{A}, P_{Deps} | N \geq N^*)$ , can be seen in Figure 6a overlaid with the dashed curve of Figure 4b (the *Average Fleet Mix Throughput*). The comparison shows that the solid lines in Figure 6a are in fact the dashed line parameterized by the number of props taking off in the 15-minute interval.



(a) Regression of the takeoff rate as function of landings rate and fleet mix for  $N \geq 22$  (b) Average throughput and capacity envelope comparison

Figure 6: BOS departure throughput in segment (VMC ; 22L, 27 | 22L, 22R) using different estimation methods

From Figure 6a, we observe the following:

- The average departure throughput curve is close to that corresponding to a fleet mix of 1 prop taking off in a 15 minute interval. This is consistent with the number of props in the fleet mix at BOS, which was around 10% in 2007.
- The number of props has a significant impact on the departure throughput. In the most common operating scenarios in which the rate of arrivals is 5-10 aircraft/15 min and the number of props is 0-2, the departure throughput increases at a rate of almost one for each additional prop.
- From this plot and other statistical analyses, we conclude that for this runway configuration at BOS, the fleet mix is a more significant explanatory variable of the departure throughput than the arrival throughput. The departure throughput decreases with the arrival throughput by at most 2.6 operations per 15 min, for an increase of arrival throughput from 0 to 14 aircraft

/15 minutes. In contrast, increasing the number of props in the fleet mix from 0 to 5 increases the departure throughput by 4.4 operations/15 min.

## 4.2 Comparison to capacity envelopes

In this section, we demonstrated how the departure throughput can be modeled as a function of the arrival throughput and the fleet mix under persistent departure demand. We showed how the average departure throughput under persistent demand (11 aircraft/15 min) can take range from 8.5 to 14.5 aircraft /min depending on the arrival throughput and the fleet mix.

A logical question is how the estimated functions plotted in Figure 6a compare to standard empirical capacity envelope estimates. Empirical capacity envelopes represent the highest departure throughput as a concave non-increasing function of the arrival throughput: The curve enveloping the observed maximum arrival and departure counts, after correcting for outliers, is considered the airport capacity envelope. For the capacity envelope estimation, we use the approach suggested by Ramanujam and Balakrishnan [5], which for this runway configuration at BOS yields the capacity envelope plotted in Figure 6b. The maximum total capacity is achieved at the point of free departures: 27 movements/ 15 minutes<sup>3</sup>. The capacity envelope is overlaid with the average departure throughput curve and the highest departure throughput curve (the one with the most favorable fleet mix). We observe that the capacity envelope is close to the throughput curve of the most favorable fleet mix. This reveals an inherent ambiguity in the analysis of the capacity envelope. While the commonly accepted definition of capacity is "the *average* number of movements that can be performed on the runway system in the presence of continuous demand" [2], most empirical capacity envelope estimation methods focus on the best-case scenario, that is, the *maximum* number of movements that can be performed on the runway system in the presence of continuous demand. These maximum counts are achievable only under special circumstances, such as a favorable fleet mix or a favorable runway sequence. In this case of BOS, the difference between the *capacity envelope* and the *average departure throughput in the presence of continuous demand* estimates for the departure capacity at a given arrival throughput can be as large as 4 operations/15 minutes.

## 4.3 Interactions between jet and prop departures

In the last section, we showed that the departure throughput increases at a rate of almost one operation per prop in the departure fleet mix. This could imply that jet and prop operations are fairly decoupled at BOS, which supports the belief of Air Traffic Controllers. In order to study the interaction of jets and props in more detail, we estimate the jet throughput under persistent jet demand as a function of arrivals and prop departures.

We isolate data points which satisfy the following two conditions:

---

<sup>3</sup>FAA calculates the capacity of this runway configuration at 28-29 movements/15 minutes [4].

- The time intervals which can be assumed to be under persistent jet departure demand.
- The time intervals for which the total departure throughput is at least as high as the highest prop throughput.

As we shall see later, the first condition is satisfied when the number of jets taxiing out is equal or higher than 17. The second condition ensures that we exclude conditions with unexpectedly low throughput. Figure 7 shows the takeoff rate of jets as a function of the landing rate and prop takeoffs. Figure 7 shows that for this runway configuration at BOS, increasing the number of props in the fleet mix decreases the takeoff rate of jets by very little. In particular, we note that the curve of the average jets throughput given 3 prop takeoffs is one unit lower than the one of the average jet throughput given 0 props. This means that on average, for the servicing of three props, one less jet will takeoff. The total departure throughput will increase by two units in agreement with the plots of Figure 6a.

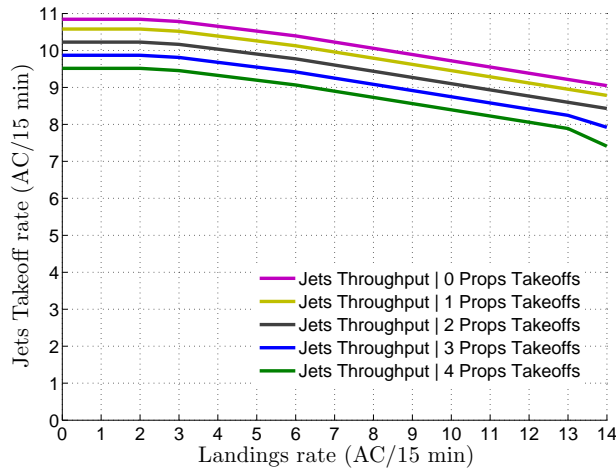


Figure 7: BOS departure throughput tradeoff between props and jets in segment (VMC ; 22L, 27 | 22L, 22R)

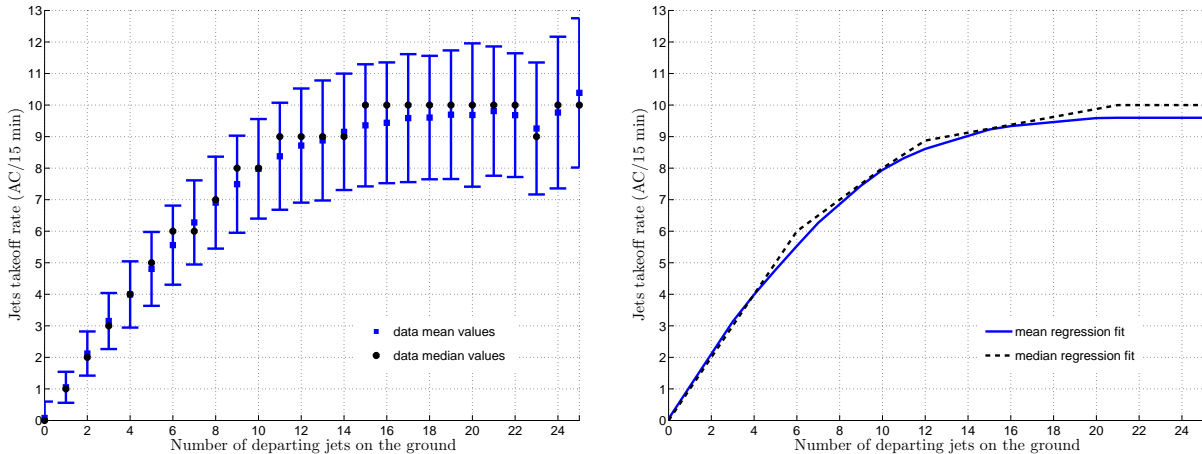
Figures 6a and 7 demonstrate that there is little interaction between jets and props for this particular runway configuration at BOS. Their operations tend to be decoupled, especially for low numbers of props in the departing mix (such as 0, 1, or 2), which are also the most frequently encountered (the mean value of prop takeoffs is 1.04 and the median 1 / 15 minutes), the reduction of the jet departure throughput is at most 0.5 operation. This validated the hypothesis of the ATC controllers that prop departures have a marginal impact on jet departure throughput. As a next step we study the departure throughput of jets only as a function of jet departure demand and arrivals, neglecting the impact of prop departures. This is essentially an approximation, but we will show that it is a sufficiently robust one.



## 5 Jet Departure Throughput

For this section, we use the whole dataset excluding all prop departures. As a first step we generate the average throughput curves, similarly to Section 2: The jet departure demand,  $N_J$ , at some minute  $t$  is measured as the number of jets taxiing out during this minute. The jet departure throughput during a 15-minute period starting at time  $t$  is defined as the jet takeoff rate,  $\bar{T}_j$  over this time period and is measured as the number of jets that took off during the 15-minute interval  $[t, t + 14]$  min.

This representation yields the plots of Figure 8a, in which we plot the mean and median jet takeoff rate for each value of the jet departure demand,  $N_J$ . The error bars depict the standard deviation of the takeoff rate at each value of  $N_J$ . In Figure 8b, we show the corresponding regression fits. The mean takeoff rate saturates at 9.6 jet takeoffs/ 15 minutes when  $N_J \geq 20$  and median takeoff rate saturates at 10 when  $N_J \geq 21$ . We observe that the average jet average takeoff rate of this runway configuration under persistent demand is around 10 jet takeoffs/ 15 minutes. The fitted curves suggest that persistent demand is achieved when the number of jets taxiing out is around 20.



(a) Measurements of the jet takeoff rate as function of de- (b) Regression of the jet takeoff rate as function of depart-  
 ing jets on the ground ing jets on the ground

Figure 8: BOS jet departure throughput in segment (VMC ; 22L, 27 | 22L, 22R)

### 5.1 Estimation of the saturation point $N_J^*$

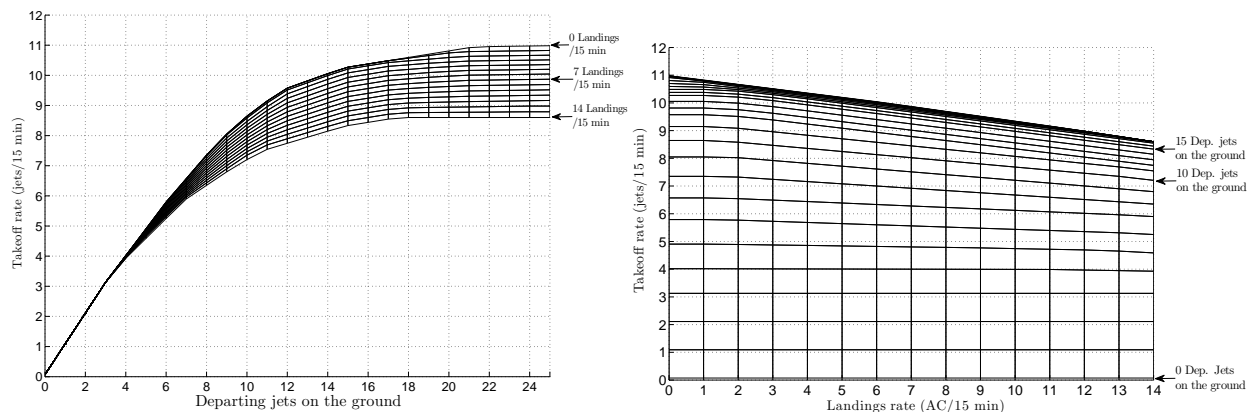
The mean and median throughput measurements and fitted curves coincide in Figure 1 in congestion, whereas they do not match in Figure 8. This discrepancy results from the approximation of excluding props. The median estimates are more robust to outliers resulting from the rare events of having a high number of props, which would lead to a reduced number of jet operations even

under high demand. The fitted curves also saturate at a very high number of  $N_J$ , in particular they saturate at  $N_J = 21$ , at only one point less than  $N^*$ . This is also a result of excluding props.

Because of the approximation of this analysis, we need a more robust way to identify  $N_J^*$ . By using Kruskal-Wallis one-way analysis of variance, we find that the measurements of throughput for different values of  $N_J$  for  $N_J \geq 17$  are not significantly different. We can conclude, that all else being equal, the jet departure throughput does not significantly vary with jet demand at demand values greater or equal than  $N_J^* = 17$ .

## 5.2 Jet departure throughput as a function of jet departure demand and arrival throughput

Using the same methodology as in Section 3, the jet takeoff rate is estimated as a function of the jet departure demand and arrival throughput. Two visualizations of the estimated function  $g$  can be seen in Figure 9. Figure 9a is essentially the mean regression curve of Figure 8b, parametrized for different levels of arrival throughput. As expected, the arrival throughput impacts the jet departure throughput. Figure 9b displays the same graph from a different angle: the arrival throughput is the variable on the  $x$ -axis and the departure demand is a parameter.



(a) Jet takeoff rate as function of departure demand

(b) Jet takeoff rate as function of landing rate

Figure 9: BOS jet departure throughput in segment (VMC ; 22L, 27 | 22L, 22R) as function of arrivals and departure demand

## 5.3 Average jet departure throughput as a function of arrival throughput and fleet mix under persistent jet departure demand

Similarly to Section 3.2, we isolate the data points for which  $N_J \geq 17$  and we estimate the average jet departure throughput as a non-increasing concave function of the arrival throughput. The fitted curve can be seen in Figure 10a in red labeled as “Jet Average Throughput”. We also plot three curves from Figure 7, namely the average jet throughput given 0,1 and 2 prop takeoffs. As a

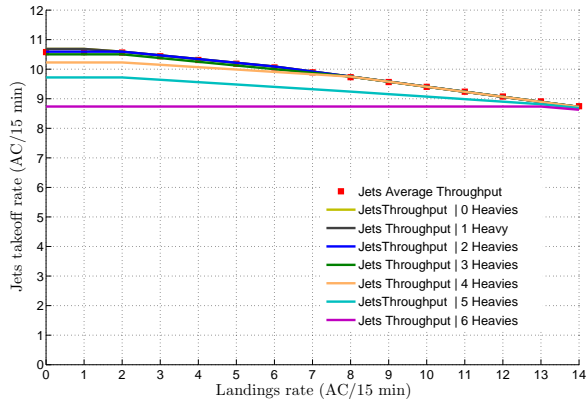
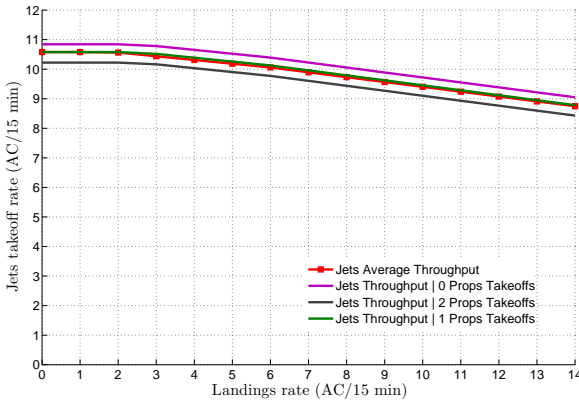
reminder, these throughput plots are fitted curves of the jet departure throughput for  $N_J \geq 17$ , parametrized for the number of prop takeoffs. We note that the “Jet Average Throughput” curve almost coincides with the curve of “Jet Throughput | 1 Prop Takeoffs” and lies between the curves of “Jet Throughput | 0 Prop Takeoffs” and “Jet Throughput | 2 Prop Takeoffs”. This shows that estimating the jet departure throughput after neglecting all prop operations does not bias the estimation. Thus, by studying the jet departures omitting the props, the resulting jet throughput estimation is representative of the average mix between jets and props.

As a final step, we study the impact of heavy weight class departures on the jet departure throughput. We have already seen in Section 4 that they are a less significant explanatory variable of the departure throughput than the number of props and the number of arrivals. Now, we can visualize this result by representing the jet departure throughput under persistent jet demand as a function of the arrivals and the number of heavies in the jet mix taking off in a 15-minute interval. The graph of the estimated function can be seen in Figure 10b. Evidently, the jet departure throughput is insensitive to the number of heavies in the jet mix as long as the number of heavies is not higher than 3, which is the case 95% of the high demand periods at BOS. There are two final remarks in respect to Figure 10b. We see that the departure throughput when 5 heavies depart is at most 9.7 jets in 15 minutes. This is to be expected, given that a heavy departure introduces a two minute separation requirement. Thus, 5 heavy departures occupy a ten minute window leaving room for at most 5 more jets in the remaining 5 minutes. Therefore, the throughput is expected to be slightly lower than 10 jet departures in 15 minutes. Similarly, when the number of heavies is 6, the throughput is expected to be slightly lower than 9. Finally, it is not surprising that the throughput curve when there are six heavies departing is flat implying that the departure throughput is insensitive to the number of arrivals: The large number of heavies results in many long separation requirements during which practically all available arrivals can cross the departure runways.

## 6 Conclusions

In this report we showed new methods for the parametric estimation of the departure throughput and capacity of an airport. We showed that the departure throughput can be estimated and represented as a function of two variables: the departure demand and the arrival throughput. We also showed how to measure departure capacity as a function of the arrival throughput and the fleet mix.

For the case of runway configuration (22L, 27 | 22L, 22R) of BOS, we showed how the mean departure capacity (11 aircraft/15 min) can take range from 8.5 to 14.5 aircraft / 15 min depending on the arrival throughput, and the fleet mix. We also demonstrated that for this runway configuration at BOS, the fleet mix is a more significant explanatory variable of the departure throughput than the arrival throughput, and compared our results to state of the art capacity envelopes. The



(a) Jet takeoff rate as a function of landings rate and departing props for  $N_J \geq 17$  (b) BOS jets takeoff rate as a function of landings rate and departing heavies for  $N_J \geq 17$

Figure 10: Jet departure throughput in segment (VMC ; 22L, 27 | 22L, 22R) using different estimation methods

comparison suggested that capacity envelope estimates differ from our estimates primarily because traditional capacity envelopes do not consider the effect of fleet mix.

Furthermore, we presented a methodology for studying the interactions between different weight classes of aircraft. This methodology indicated that jet operations are decoupled from those props of BOS. Moreover, it showed that jet throughput does not get impacted by the share of heavy weight class jets in the mix of departing aircraft for reasonable numbers of heavy aircraft.

## References

- [1] J. Cohen. *Applied multiple regression/correlation analysis for the behavioral sciences*. Lawrence Erlbaum, 2003.
- [2] Richard de Neufville and Amedeo Odoni. *Airport Systems: Planning, Design and Management*. McGraw-Hill, 2003.
- [3] R. Koenker and K.F. Hallock. Quantile regression. *Journal of Economic Perspectives*, pages 143–156, 2001.
- [4] Mitre Corporation and Federal Aviation Administration. Airport capacity benchmark report 2004. Technical report, 2004.
- [5] V. Ramanujam and H. Balakrishnan. Estimation of Arrival-Departure Capacity Tradeoffs in Multi-Airport Systems. In *Proceedings of the 48th IEEE Conference on Decision Control*, 2009.